Effects of Lowering Symmetry on the ESR Spectra of Radical Anions of Fullerene Derivatives and the Reduction Potentials

Shunichi Fukuzumi,*,†,§ Hisahiro Mori,† Tomoyoshi Suenobu,† Hiroshi Imahori,† Xiang Gao,‡ and Karl M. Kadish*,‡

Department of Material and Life Science, Graduate School of Engineering, Osaka University, CREST, Japan Science and Technology Corporation, Suita, Osaka 565-0871, Japan, and Department of Chemistry, University of Houston, Houston, Texas 77204-5641

Received: July 3, 2000; In Final Form: August 25, 2000

Radical anions of dibenzyl adducts of C_{60}, 1,4-$(C_6H_5CH_2)_2C_{60}^{\bullet -}$ and 1,2-$(C_6H_5CH_2)_2C_{60}^{\bullet -}$, give ESR spectra which have larger g values (2.0004 and 2.0001, respectively) and much smaller line widths ($\Delta H_{msl} = 2.5$ and 3.3 G, respectively, at 213 K) than the g value (1.9984) and the ΔH_{msl} value (30.9 G at 213 K) of $C_{60}^{\bullet -}$. An even smaller ΔH_{msl} value (0.17 G) and a larger g value (2.0011) are observed for the tetrabenzyl C_{60} adduct radical anion, 1,4,10,24-$(C_6H_5CH_2)_4C_{60}^{\bullet -}$ and this is ascribed to a large splitting of the degenerate t_{1u} orbitals caused by introduction of four benzyl groups to C_{60}. In this case, a hyperfine structure, due to two nonequivalent protons of only one benzyl group ($aH_1 = 0.31$ G, $aH_2 = 0.11$ G), is observed and this is consistent with the predicted localized spin density at the C2 position next to the C1 carbon to which a benzyl group is attached. The radical anions of the mono- and bisadducts formed in the Diels−Alder cycloaddition reaction of C_{60} with 9,10-dimethylanthracene show ESR signals at different g values (2.0003 for the monoadduct and 2.0009 for the bisadduct). The relationship between lower symmetry and the ESR spectra of radical anions of various C_{60} derivatives is discussed in terms of the g values and the line widths. The energy gap (δ) between the singly occupied orbital and the two other orbitals which had a t_{1u} symmetry prior to introduction of addends to C_{60} is derived from differences in the g values of various $C_{60}^{\bullet -}$ derivatives from the free spin value (2.0023). A linear correlation is shown to exist between log ΔH_{msl} and $-\delta$. The δ values are also obtained from Arrhenius plots of ln ΔH_{msl} vs T^{-1} and they agree well with the values derived from the g values and the reduction potentials.

Introduction

Buckminsterfullerene, C_{60}, has I_h symmetry and the t_{1u} of the lowest unoccupied molecular orbital (LUMO) and t_{1g} LUMO+1 orbital are both 3-fold degenerate.[1,2] The addition of one electron into the 3-fold degenerate LUMO gives a species whose ESR spectrum shows a very broad signal with a g value (1.9984) which is significantly lower than the free spin value (2.0023).[3−8] The unusually low g value of $C_{60}^{\bullet -}$ is attributed to spin−orbit coupling effects from unquenched angular momentum in Jahn−Teller distorted states of the t_{1u}^1 configuration.[3−8] The small Jahn−Teller splitting results in fast spin−lattice relaxation rates which has been the main determinant of the larger line width of $C_{60}^{\bullet -}$ with increasing temperature.[3−8] The broad ESR signal of $C_{60}^{\bullet -}$ is accompanied by a sharp spike signal, the chemical identity of which has been the major unresolved problem in $C_{60}^{\bullet -}$ ESR spectroscopy.[3−8] The most likely candidate has been suggested to be $C_{120}O^{\bullet -}$ or $(C_{60})_2^{\bullet -}$.[1] A comparison of ESR spectra of the radical anion of isolated $C_{120}O$ with the spike signal has recently provided convincing evidence for assignment of the spike signal to $C_{120}O^{\bullet -}$,[9] the neutral form of which is an ubiquitous impurity in air-exposed samples of C_{60}.[10] The symmetry of derivatized C_{60} radical anions is reduced from that of $C_{60}^{\bullet -}$, and this is expected to affect the ESR spectra. The derivatization will sufficiently perturb the $(t_{1u})^1$ degeneracy such that the line width is neither broad nor temperature dependent in contrast with the parent $C_{60}^{\bullet -}$.[11] In this context, we have recently reported that there is a splitting of the degenerate LUMO and LUMO+1 C_{60} orbitals by addition of benzyl groups to C_{60} which gives ESR spectra of the organofullerene radical anions being quite different from those of the parent C_{60} radical anion.[11] However, there has so far been no systematic study as to the effects of lowering symmetry on the ESR spectra of radical anions of fullerene derivatives.

A series of dialkyl and tetraalkyl derivatives of C_{60} which have a variety of different symmetries have been synthesized by the reactions of C_{60}^{2-} with alkyl halides.[12−16] The radical anions of these organofullerenes can be quantitatively formed by a photochemical reaction in the presence of the dimeric 1-benzyl-1,4-dihydronicotinamide $[(BNA)_2]$[17] or by a one-electron reduction of the organofullerene with tetramethylsemiquinone radical anion.[13] We have now performed a systematic study on how the lower symmetry of organofullerenes (Figure 1) will affect the ESR spectra and the reduction potentials for a series of compounds in their radical anion form and these data are compared to those of the parent C_{60} radical anion.

Experimental Section

Materials. C_{60} (>99.95% pure) was purchased from Science Laboratories Co., Ltd., Japan, and used as received. Benzonitrile

---

* Authors to whom correspondence should be addressed.

† Osaka University.

‡ University of Houston.

§ E-mail: fukuzumi@ap.chem.eng.osaka-u.ac.jp.

‖ E-mail: KKadish@uh.edu.

10.1021/jp002375c CCC: $19.00

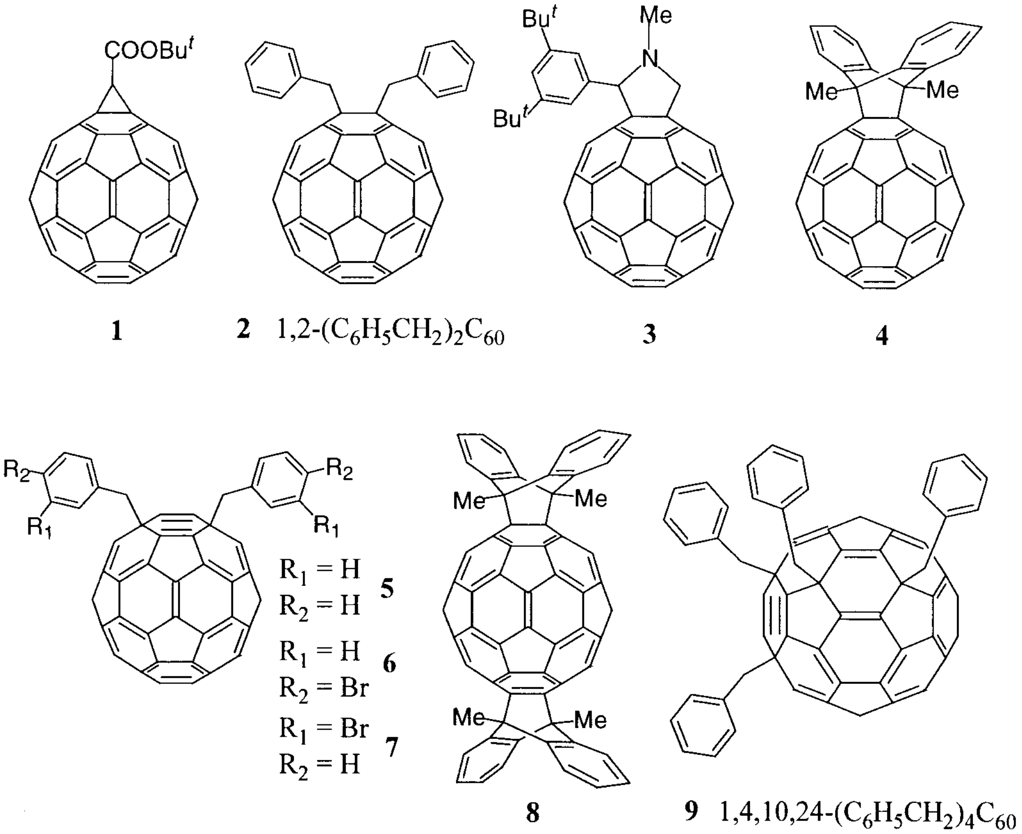

1 **2** 1,2-$(C_6H_5CH_2)_2C_{60}$ **3** **4** **5** **6** **7** **8** **9** 1,4,10,24-$(C_6H_5CH_2)_4C_{60}$

Figure 1. Various C_{60} derivatives which were examined as to the ESR spectra of the corresponding radical anions.

(PhCN) was purchased from Wako Pure Chemical Ind. Ltd., Japan, and distilled over P_2O_5 prior to use.[18] All alkyl halides, naphthalene, 9,10-dimethylanthracene, and sodium were obtained commercially. CS_2, hexane, toluene, methanol, and silica gel from EM Science (Gibbstown, NJ) were used without further treatment. Tetra-*n*-butylammonium perchlorate (TBAP) was recrystallized from ethanol and dried under vacuum at 313 K. The dimeric 1-benzyl-1,4-dihydronicotinamide [$(BNA)_2$] was prepared according to procedures described in the literature.[17,19]

The examined 1,2-$(C_6H_5CH_2)_2C_{60}$ (**2**)[20] and 1,4-R_2C_{60} derivatives (R = $C_6H_5CH_2$ (**5**), 4-$BrC_6H_4CH_2$ (**6**), 3-$BrC_6H_4CH_2$ (**7**))[12,13] were prepared by a reaction of electrogenerated $C_{60}{}^{2-}$ with RBr as described previously. This method was also utilized to prepare 1,4,10,24-$(C_6H_5CH_2)_4C_{60}$ (**9**) starting from 1,4-$(C_6H_5CH_2)_2C_{60}$.[16] The reaction between electrogenerated 1,4-$(C_6H_5CH_2)_2C_{60}{}^{2-}$ and $C_6H_5CH_2Br$ in benzonitrile was allowed to proceed for 60 min. Benzonitrile was removed from the solution by a rotary evaporator after which the solid residue was washed with methanol and filtered to eliminate the TBAP supporting electrolyte and excess $C_6H_5CH_2Br$. The crude solid was mixed with a hexanes/toluene mixture (55:45 v/v) and then analyzed by HPLC. Some material could not be eluted with the hexane/toluene mixture and required pure toluene to be eluted. The crystal structure of one fraction eluted with the hexane/toluene mixture was determined to be the 1,4;1,4-isomer of $(C_6H_5CH_2)_4C_{60}$, which is designated as 1,4,10,24-$(C_6H_5CH_2)_4C_{60}$ (**9**).[16] The C_{60} monoadduct (**4**) and bisadduct (**8**) of 9,10-dimethylanthracene were prepared by the reaction of C_{60} (2.8×10^{-4} M) with 9,10-dimethylanthracene (2.8×10^{-4} or 2.8×10^{-3} M) at room temperature in benzonitrile. The product mixtures for measurements of FAB-mass spectra were obtained by the simple evaporation of the solvents. The [6,6]-methanofullerene (**1**)[21] and the C_{60}-*N*-methylpyrrolidine derivative (**3**)[22] were synthesized according to literature procedures.

ESR Measurements. A quartz ESR tube (4.5-mm i.d.) containing a deaerated benzonitrile solution of $(BNA)_2$ (1.0×10^{-4} M) and C_{60} (2.0×10^{-4} M) was irradiated in the cavity of the ESR spectrometer with the focused light of a 1000-W high-pressure Hg lamp through an aqueous filter. The radical anion of 1,4,10,24-$(C_6H_5CH_2)_4C_{60}$ (2.8×10^{-4} M) was also produced by photochemical reduction of tetrabenzyl C_{60} adduct with $(BNA)_2$ (1.4×10^{-3} M). The ESR spectra in frozen benzonitrile were measured at various temperatures (133 to 233 K) with a JEOL X-band spectrometer (JES-RE1XE) using an attached VT (variable temperature) apparatus. More concentrated benzonitrile solutions of $C_{60}{}^{\bullet -}$ were needed for the ESR measurements of $C_{60}{}^{\bullet -}$ at higher temperatures, and these were produced with the reduction of C_{60} by tetramethyl-semiquinone radical anion, which was used to determine the large line widths. Typically, an aliquot of tetramethylsemiquinone radical anion (4.0×10^{-3} M) was added to a quartz cuvette (10 mm i.d.) which contained a deaerated PhCN suspension (3.0 mL) of C_{60} (4.0×10^{-3} M) under an atmospheric pressure of Ar. Tetra-*n*-butylammonium hydroxide (TBAOH) was used for generation of the tetramethylsemiquinone radical anion in the reaction between tetramethylhydroquinone and tetramethyl-*p*-benzoquinone.[13] After addition of tetramethylsemiquinone radical anion, the suspension of C_{60} became soluble in benzonitrile where $C_{60}{}^{\bullet -}$ (4.0×10^{-3} M) was formed quantitatively. The deaerated benzonitrile solution of $C_{60}{}^{\bullet -}$ was transferred to a quartz ESR tube (1.2 mm i.d.) with a microsyringe under an atmospheric pressure of Ar. The small i.d. size is required because of the large dielectric loss of benzonitrile solution. The radical anions of 1,4- and 1,2-R_2C_{60} as well as C_{60}-anthracene adducts were also produced by the tetramethyl-semiquinone radical anion.[13] The ESR spectra were recorded under nonsaturating microwave power conditions. The magnitude of modulation was chosen to optimize the resolution and the signal-to-noise (*S*/*N*) ratio of the observed spectra, when the maximum slope line width (ΔH_{msl}) of the ESR signals was unchanged with larger modulation. The *g* values and hyperfine coupling constants were calibrated precisely with an Mn^{2+} marker which was used as a reference.

Theoretical Calculations. Theoretical calculations were performed using the MOPAC program (Version 6) which is incorporated in the MOLMOLIS program by Daikin Industries, Ltd. The PM3 Hamiltonian was used for the semiempirical MO calculations.[23] Final geometries and energetics were obtained by optimizing the total molecular energy with respect to all structural variables. The heats of formation (ΔH_f) were calculated with the restricted Hartree−Fock (RHF) formalism using a key word "PRECISE".

Results and Discussion

ESR Spectra of Radical Anions of C_{60} Derivatives. The radical anion of C_{60} is quantitatively formed by the photochemical reaction of C_{60} with dimeric 1-benzyl-1,4-dihydronicotinamide [$(BNA)_2$] which acts as an electron donor in PhCN (eq 1).[17] The ESR spectrum of $C_{60}^{\bullet-}$ (Figure 2a) thus formed shows a characteristic broad signal of $C_{60}^{\bullet-}$ ($g = 1.9984$, $\Delta H_{\mathrm{msl}} = 30.9$ G) at 213 K together with a sharp "spike" signal ($g = 2.0002$, $\Delta H_{\mathrm{msl}} = 2.0$ G) which is always seen in the ESR spectrum of $C_{60}^{\bullet-}$.[3−8,25,26]

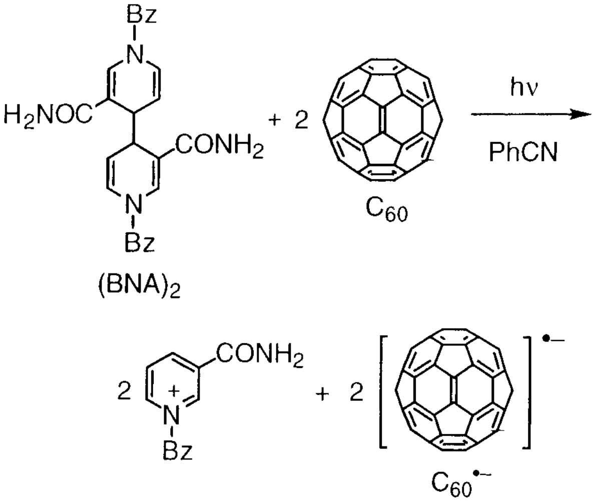

(1)

The ESR spectrum of the radical anion of 1,2-$(C_6H_5CH_2)_2C_{60}$ (**2**), which has a lower symmetry (C_{2v}) as compared to the I_h symmetry of C_{60},[20] shows a much sharper signal and has a larger *g* value ($g = 2.0001$, $\Delta H_{\mathrm{msl}} = 3.9$ G) in PhCN at 298 K than $C_{60}^{\bullet-}$ at 213 K and this is illustrated in Figure 2b. Essentially the same ESR spectrum ($g = 2.0001$, $\Delta H_{\mathrm{msl}} = 3.3$G) was observed in frozen PhCN at 173 K. Hyperfine structure due to the methylene protons of the benzyl groups is not observed, even at a much smaller modulation (0.2 G) and this could be due to the fact that the hyperfine coupling constants may be too small to detect with this line width (3.3 G). When the symmetry is further reduced from C_{2v} in 1,2-$(C_6H_5CH_2)_2C_{60}$ (**2**) to C_s in 1,4-$(C_6H_5CH_2)_2C_{60}$ (**5**),[20] the ESR spectrum of 1,4-$(C_6H_5CH_2)_2C_{60}^{\bullet-}$ gives a slightly larger *g* value and a smaller line width ($g = 2.0004$, $\Delta H_{\mathrm{msl}} = 2.5$ G) than is seen for 1,2-$(C_6H_5CH_2)_2C_{60}^{\bullet-}$.

Figure 3 shows plots of the line width (ΔH_{msl}) for the broad signal of $C_{60}^{\bullet-}$ and the sharp signals of 1,4-$(C_6H_5CH_2)_2C_{60}^{\bullet-}$ (**5**$^{\bullet-}$) and 1,2-$(C_6H_5CH_2)_2C_{60}^{\bullet-}$ (**2**$^{\bullet-}$) as a function of temperature. The ΔH_{msl} value of $C_{60}^{\bullet-}$ in frozen benzonitrile increases significantly with temperature as was earlier reported,[3−8,] whereas the ΔH_{msl} values of 1,4-$(C_6H_5CH_2)_2C_{60}^{\bullet-}$ (2.5 G) and 1,2-$(C_6H_5CH_2)_2C_{60}^{\bullet-}$ (3.3 G) remain nearly constant below 213 K, irrespective of temperature. The broad ESR signal, the temperature dependence of ΔH_{msl} for $C_{60}^{\bullet-}$ and its small *g* value as compared to the free spin value (2.0023) have been ascribed to a degenerate $^2E_{1u}$ ground state and a low-lying $^2A_{2u}$ excited state, both of which would arise from Jahn−Teller distortion of $C_{60}^{\bullet-}$ along the principal axis in D_{5d} symmetry.[3−8,26,27] Since 1,4-$(C_6H_5CH_2)_2C_{60}$ and 1,2-$(C_6H_5CH_2)_2C_{60}$ have a much lower symmetry (C_s and C_{2v}, respectively), the triply degenerate t_{1u} orbitals in the parent C_{60} would no longer be degenerate in 1,4- and 1,2-$(C_6H_5CH_2)_2C_{60}$. The line widths of 1,4-$(C_6H_5CH_2)_2C_{60}^{\bullet-}$ (**5**$^{\bullet-}$) and 1,2-$(C_6H_5CH_2)_2C_{60}^{\bullet-}$ (**2**$^{\bullet-}$) therefore become much smaller than that of $C_{60}^{\bullet-}$, while the *g* values (2.0004 and 2.0001, respectively) become larger than that of $C_{60}^{\bullet-}$ ($g = 1.9984$).

Radical anions of other 1,2- and 1,4-adducts of C_{60} (Figure 1) were also prepared by the one-electron reduction of these organofullerene with tetramethylsemiquinone radical anion. The

(a) $C_{60}^{\bullet-}$

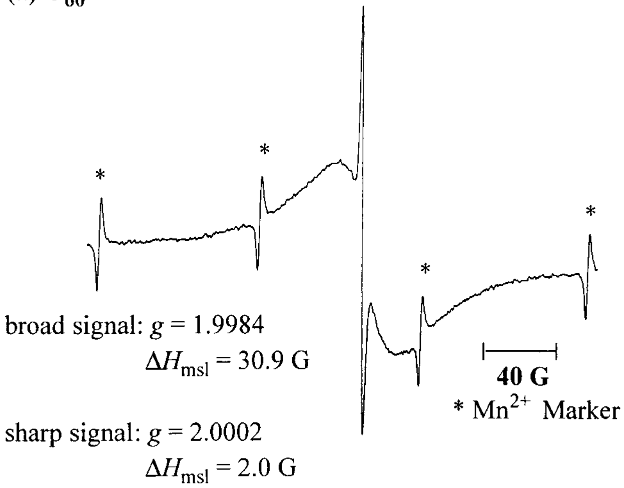

(b) 1,2-$(C_6H_5CH_2)_2C_{60}^{\bullet-}$ ($2^{\bullet-}$)

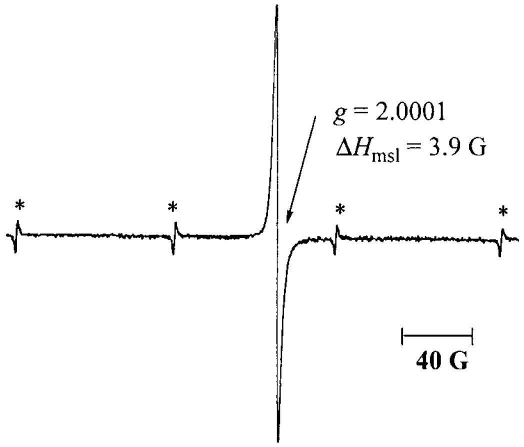

Figure 2. ESR spectra of (a) $C_{60}^{\bullet-}$ generated in the photoinduced electron transfer from $(BNA)_2$ (1×10^{-4} M) to C_{60} (2×10^{-4} M) in deaerated PhCN observed at 213 K under irradiation of UV−Vis light from a Xe lamp, and (b) 1,2-$(C_6H_5CH_2)_2C_{60}^{\bullet-}$ generated in the electron-transfer reduction of 1,2-$(C_6H_5CH_2)_2C_{60}$ (2×10^{-4} M) by tetramethylsemiquinone radical anion (2×10^{-4} M) in deaerated PhCN observed in benzonitrile at 298 K. Asterisk (*) denotes an Mn^{2+} marker.

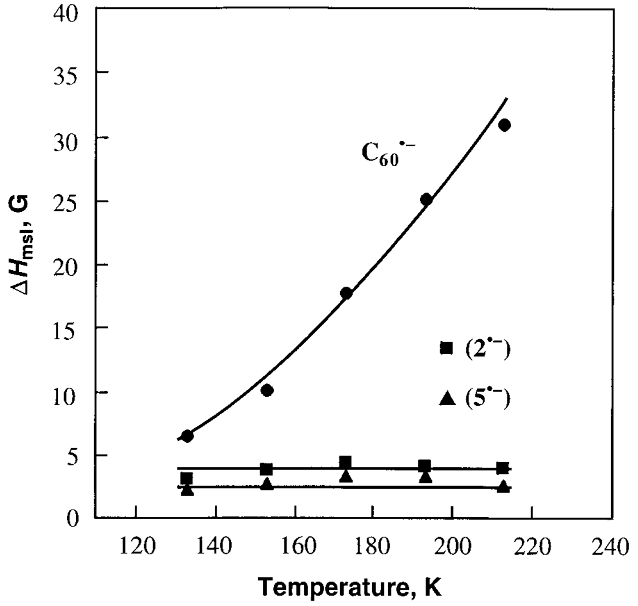

Figure 3. Temperature dependence of ΔH_{msl} of ESR spectra for $C_{60}^{\bullet-}$ (●), 1,2-$(C_6H_5CH_2)_2C_{60}^{\bullet-}$ (■), and 1,4-$(C_6H_5CH_2)_2C_{60}^{\bullet-}$ (▲) in frozen benzonitrile.

TABLE 1: The Isotropic *g*-Values and Line Width (ΔH_{msl}) of the ESR Signals of Radical Anions of C_{60} and Derivatives, the Energy Gap (δ) between the LUMO and LUMO+1 Orbitals, and the Difference in the First and Third Reduction Potentials in Reference to C_{60} (ΔE_{1-3})

	g-value	ΔH_{msl} (G)	δ^a (kcal mol^{-1})	δ^b (kcal mol^{-1})	$\Delta E_{1-3}{}^c$ (kcal mol^{-1})
C_{60}	1.9984	60.0	1.0	1.0	–
1	1.9998	4.1	1.6	1.7	0.5
2	2.0001	3.9	1.8	1.8	0.7
3	2.0002	1.7	1.9		
4	2.0003	1.5	2.0	1.9	
5	2.0004	2.5	2.1		1.6
6	2.0007	0.9	2.5	2.6	2.5
7	2.0008	0.8	2.7	2.6	2.3
8	2.0009	0.4	2.9	2.9	
9	2.0010	0.2	3.1		6.7
"Spike"	2.0002	1.1	1.9	1.3	

[a] Derived from the *g*-values using eq 3. [b] Derived from the temperature dependence of ΔH_{msl} using eq 4. [c] Obtained from the reduction potentials in refs 14−16, 20.

g values and ΔH_{msl} values obtained from the ESR spectra of these radical anions recorded at 298 K are listed in Table 1. In general, larger *g* values and smaller line widths are obtained for radical anions of the 1,4-adducts than those of the 1,2-adducts. This is consistent with the lowered symmetry of the 1,4-adducts (C_s) as compared to the C_{2v} symmetry of the 1,2-adducts and is seen for all investigated compounds except for 1,4-$(C_6H_5CH_2)_2C_{60}^{\bullet-}$ (**5**) which has a larger ΔH_{msl} value than 1,2-adduct radical anions (**3**, **4**).

The introduction of two additional benzyl addends to the dibenzyl adduct of C_{60} may result in a much larger splitting of the triply degenerate t_{1u} orbitals than is seen in the case of the parent C_{60}. An X-ray structure of the major product which was isolated in a reaction of the dianion of 1,4-$(C_6H_5CH_2)_2C_{60}$ with $C_6H_5CH_2Br$ reveals formation of 1,4,10,24-$(C_6H_5CH_2)_4C_{60}$ (**9**) which has no symmetry (C_1).[16]

The radical anion of 1,4,10,24-$(C_6H_5CH_2)_4C_{60}$ produced by the photochemical reaction of 1,4,10,24-$(C_6H_5CH_2)_4C_{60}$ with $(BNA)_2$ exhibits a much sharper ESR signal as compared to 1,4-$(C_6H_5CH_2)_2C_{60}^{\bullet-}$.[12] The *g* value of 2.0010 for 1,4,10,24-$(C_6H_5CH_2)_4C_{60}^{\bullet-}$ ($\mathbf{9}^{\bullet-}$) becomes closer to the free spin value ($g = 2.0023$) and is quite different from the *g* value of $C_{60}^{\bullet-}$ ($g = 1.9984$). The hyperfine structure with $a\mathrm{H}_1 = 0.31$ G, $a\mathrm{H}_2 = 0.11$ G is observed with the smallest line width ($\Delta H_{msl} = 0.17$ G) among the organofullerene radical anions in Table 1.[12] The much smaller ΔH_{msl} value (0.17 G) and larger *g* value (2.0011) of 1,4,10,24-$(C_6H_5CH_2)_4C_{60}^{\bullet-}$ as compared to $C_{60}^{\bullet-}$ ($\Delta H_{msl} = 30.9$ G and $g = 1.9984$) are ascribed to a large splitting of the degenerate t_{1u} orbitals caused by introduction of four benzyl groups to C_{60}. The hyperfine structure arises from interaction of the single unpaired electron with two nonequivalent protons of only one of the four benzyl groups in 1,4,10,24-$(C_6H_5CH_2)_4C_{60}^{\bullet-}$.[12]

SCHEME 1

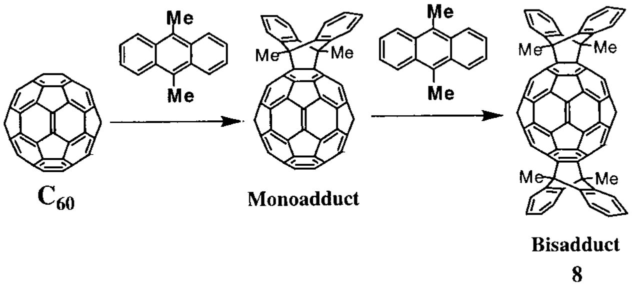

The Diels−Alder reactions of C_{60} with anthracene and substituted anthracenes are known to undergo [4+2] cycloaddition where not only the C_{60}-anthracene 1:1 cycloadduct, i.e., the monoadduct, but also the 1:2 adduct (the bisadduct) are formed as a mixture at ambient temperature in solution (Scheme 1).[28] In the same manner, a product mixture of monoadduct and bisadduct was obtained in the solvent-free reaction of C_{60} with 9-methylanthracene.[29] Only the monoadduct is formed in the Diels−Alder reaction of C_{60} (2.8×10^{-4} M) with one equivalent of 9,10-dimethylanthracene (2.8×10^{-4} M) in PhCN for 1 h at 298 K. As the reaction proceeds, the diagnostic visible absorption band of the 1,2-adduct appears as a sharp peak at $\lambda_{max} = 434$ nm. The monoadduct can be reduced by the addition of one equivalent of tetramethylsemiquinone radical anion to form the monoadduct radical anion and corresponding quinone (eq 2).

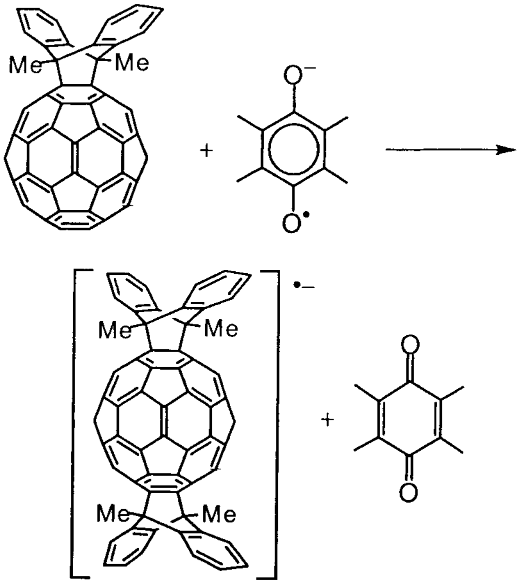

(2)

The radical anion of the monoadduct ($\mathbf{4}^{\bullet-}$) shows a NIR band at $\lambda_{max} = 1030$ nm which is the diagnostic absorption band for

(a) Monoadduct $4^{\bullet-}$

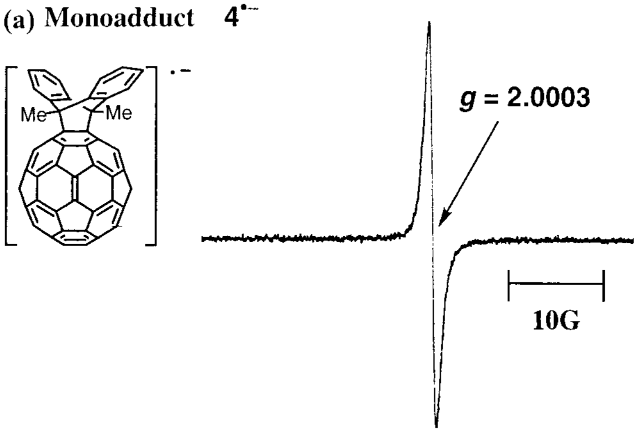

(b) Bisadduct + Monoadduct

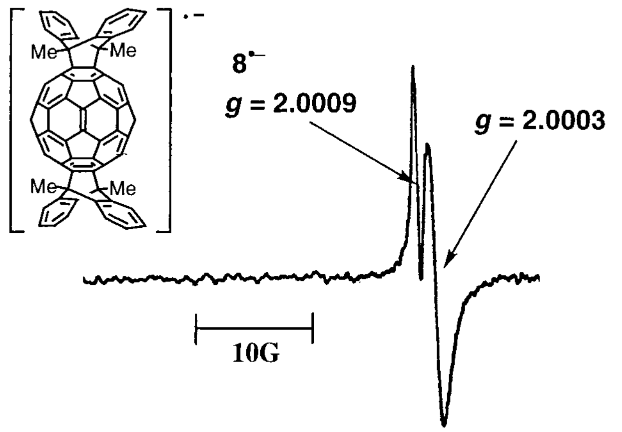

Figure 4. ESR spectra of radical anions of C_{60}-9,10-dimethylanthracene (a) monoadduct and (b) a mono- and bisadduct mixture.

the radical anions of 1,2-R_2C_{60} where R = $PhCH_2$, Me, or *o*-xylyl.[20] The ESR spectrum of the monoadduct radical anion shows a sharp isotropic signal (ΔH_{msl} = 1.3 G) with no hyperfine at g = 2.0003 as shown in Figure 4a. Such narrow ESR signals at small g values are characteristic of the 1,2-adduct radical anions as observed in the case of 1,2-$(PhCH_2)_2C_{60}^{\bullet-}$ (**5**$^{\bullet-}$, vide supra), and this indicates that the cycloaddition occurs at the 6,6-junction of the C_{60} skeleton to form the 1,2-adduct.

When a 10-fold excess amount of 9,10-dimethylanthracene (2.8×10^{-3} M) was added to a C_{60} (2.8×10^{-4} M) solution of PhCN, a mixture of the monoadduct and bisadduct was generated at room temperature in 1 h. Bisadduct formation was confirmed by negative ion FAB-mass spectra which gave peaks at the mass number of the monoadduct (927) and the bisadduct (1132). The ESR spectrum of the reaction mixture in PhCN (Figure 4b) shows a signal consisting of the two narrow isotropic signals with different g values (2.0009 and 2.0003). The g value at 2.0003 coincides with that for the monoadduct radical anion, whereas the larger g value (2.0009) with a narrower isotropic signal (ΔH_{msl} = 0.6 G) can be assigned to the bisadduct radical anion (see Table 1).

Determination of Energy Splitting in Organofullerene Radical Anions. The extensive data in Table 1 allow a correlation to be made between the g values and the ΔH_{msl} values of the examined organofullerene radical anions. The deviation of g values of these organofullerene radical anions from the free spin value (g_e = 2.0023) can be expressed in terms of the spin−orbit coupling constant of the carbon atom (ξ) and the energy gap (δ) between the singly occupied orbital and the two other orbitals as given by eq 3.[26] A constant (C) is a value determined by the coefficients of SOMO (singly

$$g = g_e - C\xi/\delta \tag{3}$$

occupied MO) and LUMO orbitals of organofullerene radical anions.[26]

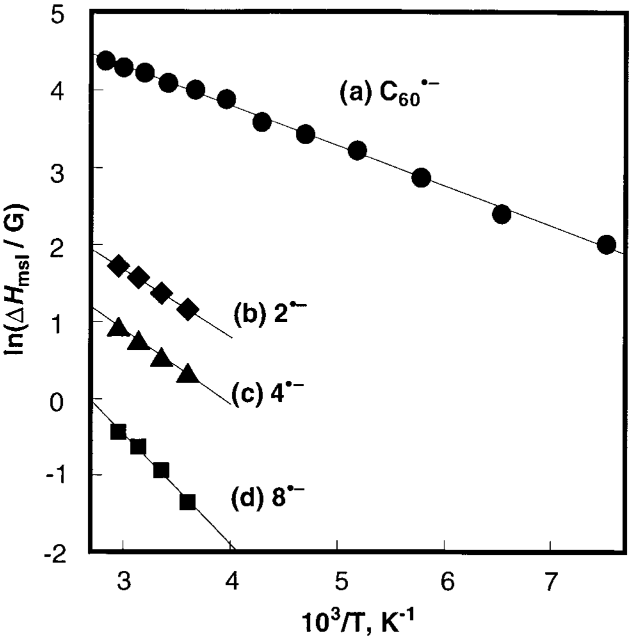

Figure 5. Plots of ln ΔH_{msl} vs T^{-1} for (a) $C_{60}^{\bullet-}$, (b)−(d) derivatized C_{60} radical anions (**2**, **4**, **8**).

A t_{1u} orbital splitting of $C_{60}^{\bullet-}$ results from the Jahn−Teller distortion.[3−8,26,27] The δ value due to the Jahn−Teller distortion has been theoretically estimated to be small (190 cm^{-1}), corresponding to 0.54 kcal mol^{-1}.[30] This means a low-lying excited-state exists in $C_{60}^{\bullet-}$. In such a case, the line width is mainly determined by an Orbach spin−lattice relaxation process.[31] The Orbach relaxation rate which is proportional to the line width (ΔH_{msl}) is given by eq 4, which agrees with the experimental observation for

$$\Delta H_{msl} \propto \exp(-\delta/\mathrm{RT}) \tag{4}$$

the temperature dependence of ΔH_{msl} of the ESR spectra of $C_{60}^{\bullet-}$ in the temperature range between 70 and 300 K.[27,32] The δ value for powder samples of tetraphenylphosphonium chloride salt of $C_{60}^{\bullet-}$, $(Ph_4P^+\ C_{60}^{\bullet-})\bullet 2(Ph_4P^+Cl_x^-)$, has been determined as 0.43 kcal mol^{-1} (152 cm^{-1}),[27] in reasonable agreement with the theoretical expectation.[30]

According to eq 4, a linear correlation should be obtained between ln ΔH_{msl} and T^{-1}. The temperature dependence of ΔH_{msl} of $C_{60}^{\bullet-}$ was examined in the temperature range higher than the melting point of benzonitrile up to 353 K. Accurate determination of the large ΔH_{msl} values of $C_{60}^{\bullet-}$ in solution at high temperatures is difficult due to the low solubility of C_{60} in PhCN.[33] To obtain a sufficient signal intensity for accurate determination of the ΔH_{msl} values, we have used a large amount of C_{60} (3.9×10^{-3} M) which was suspended in benzonitrile. The C_{60} radical anion is more soluble than C_{60} itself and after the reduction with tetramethylsemiquinone radical anion, the resulting $C_{60}^{\bullet-}$ became completely soluble in benzonitrile (see Experimental Section). A linear plot of ln ΔH_{msl} vs T^{-1} for $C_{60}^{\bullet-}$ in benzonitrile is obtained in the wide temperature range as shown in Figure 5a. In the case of $C_{60}^{\bullet-}$ in methyl-THF, the electron spin relaxation rate has been reported to show a

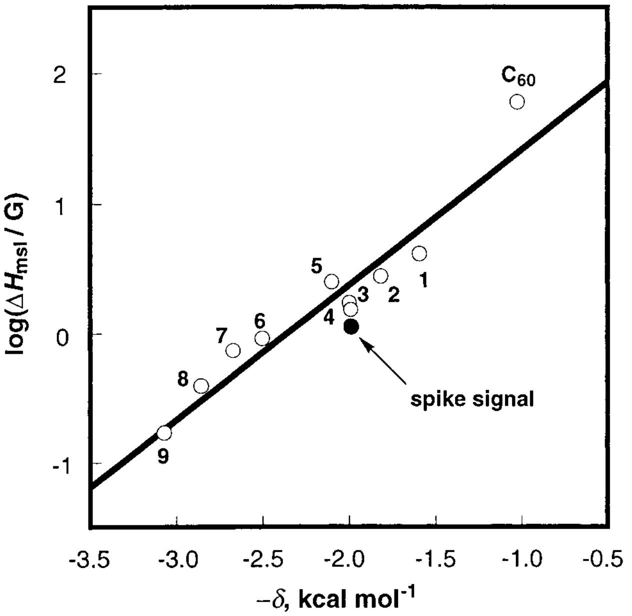

Figure 6. A plot of log ΔH_{msl} vs $-\delta$ for organofullerene radical anions (the data are taken from Table 1). The numbers refer to organofullerenes in Table 1.

temperature dependence where the relaxation reaches a plateau at higher temperatures between 200 and 290 K.[33] Such temperature dependence is characteristic of a thermally activated process. However, the present results on $C_{60}^{\bullet-}$ in benzonitrile (Figure 5a) show no leveling off of ΔH_{msl} at high temperatures up to 353 K, which is consistent with an Orbach process. From the slope, the δ value was determined as 350 cm^{-1} (1.0 kcal mol^{-1}) which is larger than the reported value of the powder sample (152 cm^{-1}).[27] This indicates that the t_{1u} degeneracy is further removed by interaction with the polar solvent resulting in a larger δ value than the value of the powder sample and the theoretical expectation.

The $C\xi$ value in eq 3 can be calculated as 1.37 cm^{-1} from the g and δ value (350 cm^{-1}) of $C_{60}^{\bullet-}$. The δ values of organofullerene radical anions can then be evaluated from the g values using eq 3 and these values are also listed in Table 1. At a constant temperature, eq 4 is rewritten by eq 5, which predicts a linear correlation between log ΔH_{msl} and $-\delta$. This correlation is confirmed as shown in Figure 6, where log ΔH_{msl} is

$$\log \Delta H_{msl} \propto -\delta/(2.3RT) \qquad (5)$$

linearly correlated with $-\delta$ which is derived from the deviation of the g values from the free spin value (eq 3). The ΔH_{msl} and $-\delta$ values of the spike signal which accompanies the broad signal of $C_{60}^{\bullet-}$ (Figure 1a) are also included in Figure 6. The data point for the spike signal fits well a correlation between log ΔH_{msl} and $-\delta$ for radical anions of C_{60} derivatives in Figure 6. This supports the idea that extrinsic factors such as $C_{120}O^{\bullet-}$, which is a ubiquitous impurity in air-exposed samples of C_{60},[10] rather than intrinsic properties of discrete $C_{60}^{\bullet-}$ are responsible for the sharp spike signal.[3,9,34]

The temperature dependence of ΔH_{msl} of a variety of derivatized C_{60} radical anions was also examined in the temperature range beyond the melting point of benzonitrile and typical plots of ln ΔH_{msl} vs T^{-1} are shown in Figure 5b−d. It is clearly shown that the ΔH_{msl} values of derivatized C_{60} radical anions (Figure 5b−d) are significantly more sensitive to the temperature than those of $C_{60}^{\bullet-}$ (Figure 5a), leading to the larger δ values than $C_{60}^{\bullet-}$. In frozen benzonitrile, however, the ΔH_{msl} values of 1,2- and 1,4-$(PhCH_2)_2C_{60}^{\bullet-}$ are insensitive to the temperature, in contrast to the case of $C_{60}^{\bullet-}$ whose ΔH_{msl} value increases with increasing the temperature (Figure 3). This apparent contradiction is attributed to an additional inhomogeneous width for derivatized C_{60} radical anions caused by the g-factor anisotropy in frozen medium, which masks the temperature dependence of ΔH_{msl} due to an Orbach spin−lattice relaxation. In the case of $C_{60}^{\bullet-}$, the anisotropy is not observed due to efficient dynamic averaging of ellipsoidal structures to give effective icosahedral symmetry (so-called pseudorotation) over the temperature range shown in Figure 2.[8,35] The δ values obtained from the slopes of linear plots of ln ΔH_{msl} vs T^{-1} using eq 4 are listed in Table 1, and agree well with the values derived from the g values using eq 3.

Splitting of the degenerate LUMO and LUMO+1 C_{60} orbitals by introduction of addends onto C_{60} should also affect the potential difference between the first and the third reduction, since the LUMO orbital can accommodate two electrons. The potential differences (ΔE_{1-3}) of derivatized C_{60} in reference to C_{60} are obtained from the reduction potentials of C_{60} and C_{60} derivatives,[14−16,20] and the ΔE_{1-3} values are also listed in Table 1. The ΔE_{1-3} values may correspond to the δ values in eq 4, since the effects of electron repulsion are largely canceled out in ΔE_{1-3} which results mainly from the orbital splitting caused by introduction of addends. Considering the experimental uncertainties (±0.02 V) in the reduction potentials, the ΔE_{1-3} values are consistent with the δ values derived from the temperature dependence of the ΔH_{msl} values (eq 4) and deviation of the g values from the free spin values (eq 3).

The calculated LUMO and LUMO+1 energies in [6,6]-methanofullerene (**1**), 1,2-$(PhCH_2)_2C_{60}$ (**2**), and 1,4,10,24-$(C_6H_5CH_2)_4C_{60}$ (**9**) confirm the splitting of the degenerate LUMO and LUMO+1 orbitals by introduction of addends. The PM3 semiempirical MO method was used to obtain the LUMO and LUMO+1 energies (see Experimental Section), since the optimized structure of **9** has been shown to agree well with the X-ray structure.[12,16] The difference in the LUMO and LUMO+1 energies increases in the following order: **1** (2.0 kcal mol^{-1}), **2** (2.8 kcal mol^{-1}), and **9** (5.1 kcal mol^{-1}), consistent with the order of δ values (1.6 kcal mol^{-1}, 1.8 kcal mol^{-1}, and 3.1 kcal mol^{-1}). Thus, the PM3 calculations are useful to predict the order of magnitude of the δ values.[36]

In summary, the present study has clarified quantitatively how a lower symmetry of C_{60} by introduction of addends affects the g values and the temperature dependence of the ΔH_{msl} values of ESR spectra of a series of derivatized C_{60} radical anions as well as the reduction potentials as compared to the parent C_{60} radical anion.

Acknowledgment. We thank an International Scientific Research Program (11694079) from the Ministry of Education, Science, Culture and Sport, Japan, and the Robert A. Welch Foundation (K.M.K., Grant E-680) for financial support.

References and Notes

(1) Hirsch, A. *The Chemistry of the Fullerenes*; Georg Thieme Verlag: New York, 1994.

(2) (a) Haddon, R. C. *Acc. Chem. Res.* **1992**, *25*, 127. (b) Saito, S.; Oshiyama, A. *Phys. Rev. Lett.* **1991**, *66*, 2637.

(3) Reed, C. A.; Bolskar, R. D. *Chem. Rev.* **2000**, *100*, 1075.

(4) Eaton, S. S.; Eaton, G. R. *Appl. Magn. Reson.* **1996**, *11*, 155.

(5) (a) Allemand, P.-M.; Srdanov, G.; Koch, A.; Khemani, K.; Wudl, F.; Rubin, Y.; Diederich, F.; Alvarez, M. M.; Anz, S. J.; Whetten, R. L. *J. Am. Chem. Soc.* **1991**, *113*, 2780. (b) Dubois, D.; Kadish, K. M.; Flanagan,

S.; Haufler, R. E.; Chibante, L. P. F.; Wilson, L. J. *J. Am. Chem. Soc.* **1991**, *113*, 4364.

(6) (a) Greaney, M. A.; Gorun, S. M. *J. Phys. Chem.* **1991**, *95*, 7142. (b) Gasyna, Z.; Andrews, L.; Schatz, P. N. *J. Phys. Chem.* **1992**, *96*, 1525. (c) Kato, T.; Kodama, T.; Shida, T.; Nakagawa, T.; Matsui, Y.; Suzuki, S.; Shiromaru, H.; Yamauchi, K.; Achiba, Y. *Chem. Phys. Lett.* **1991**, *180*, 446.

(7) Dubois, D.; Jones, M. T.; Kadish, K. M. *J. Am. Chem. Soc.* **1992**, *114*, 6446.

(8) (a) Stinchcombe, J.; Pénicaud, A.; Bhyrappa, P.; Boyd, P. D. W.; Reed, C. A. *J. Am. Chem. Soc.* **1993**, *115*, 5212. (b) Stinchcombe, J.; Pénicaud, A.; Bhyrappa, P.; Boyd, P. D. W.; Reed, C. A. *J. Am. Chem. Soc.* **1994**, *116*, 6484.

(9) Paul, P.; Bolskar, R. D.; Clark, A. M.; Reed, C. A. *Chem. Commun.* **2000**, 1229.

(10) Taylor, R.; Barrow, M. P.; Drewello, T. *J. Chem. Saoc., Chem. Commun.* **1998**, 2497.

(11) (a) Klos, H.; Gotschy, B. *Appl. Magn. Reson.* **1996**, *11*, 171. (b) Jones, M. T.; Kadish, K. M.; Subramanian, R.; Boulas, P.; Vijayashree, M. N. *Synth. Met.* **1995**, *70*, 1341. (c) Staško, A.; Brezová, V.; Biskupič, S.; Dinse, K.-P.; Groβ, R.; Baumgarten, M.; Gügel, A.; Belik, P. *J. Electroanal. Chem.* **1997**, *423*, 131. (d) Iyoda, M.; Sasaki, S.; Sultana, F.; Yoshida, M.; Kuwatani, Y.; Nagase, S. *Tetrahedron Lett.* **1996**, *37*, 7987. (e) Arena, F.; Bullo, F.; Conti, F.; Corvaja, C.; Maggini, M.; Prato, M.; Scorrano, G. *J. Am. Chem. Soc.* **1997**, *119*, 789. (f) Brustolon, M.; Zoleo, A.; Agostini, G.; Maggini, M. *J. Phys. Chem. A* **1998**, *102*, 6331.

(12) Fukuzumi, S.; Suenobu, T.; Gao, X.; Kadish, K. M. *J. Phys. Chem. A* **2000**, *104*, 2908.

(13) Subramanian, R.; Kadish, K. M.; Vijayashree, M. N.; Gao, X.; Jones, M. T.; Miller, M. D.; Krause, K. L.; Suenobu, T.; Fukuzumi, S. *J. Phys. Chem.* **1996**, *100*, 16327.

(14) Fukuzumi, S.; Suenobu, T.; Hirasaka, T.; Arakawa, R.; Kadish, K. M. *J. Am. Chem. Soc.* **1998**, *120*, 9220.

(15) Kadish, K. M.; Gao, X.; Van Caemelbecke, E.; Hirasaka, T.; Suenobu, T.; Fukuzumi, S. *J. Phys. Chem.* **1998**, *102*, 3898.

(16) Kadish, K. M.; Gao, X.; Van Caemelbecke, E.; Suenobu, T.; Fukuzumi, S. *J. Am. Chem. Soc.* **2000**, *122*, 563.

(17) Fukuzumi, S.; Suenobu, T.; Patz, M.; Hirasaka, T.; Itoh, S.; Fujitsuka, M.; Ito, O. *J. Am. Chem. Soc.* **1998**, *120*, 8060.

(18) Perrin, D. D.; Armarego, W. L. F. *Purification of Laboratory Chemicals*; Butterworth-Heinemann: Oxford, 1988.

(19) Patz, M.; Kuwahara, Y.; Suenobu, T.; Fukuzumi, S. *Chem. Lett.* **1997**, 567.

(20) Kadish, K. M.; Gao, X.; Van Caemelbecke, E.; Suenobu, T.; Fukuzumi, S. *J. Phys. Chem. A* **2000**, *104*, 3878.

(21) Wang, Y.; Cao, J.; Schuster, D. I.; Wilson, S. R. *Tetrahedron Lett.* **1995**, *36*, 6843.

(22) Imahori, H.; Ozawa, S.; Ushida, K.; Takahashi, M.; Azuma, T.; Ajavakom, A.; Akiyama, T.; Hasegawa, M.; Taniguchi S.; Okada, T.; Sakata, Y. *Bull. Chem. Soc. Jpn.* **1999**, *72*, 485.

(23) Stewart, J. J. P. *J. Comput. Chem.* **1989**, *10*, 209, 221.

(24) The quantitative formation of $C_{60}^{\bullet -}$ was confirmed by the NIR spectrum of the product which has a diagnostic marker band at λ_{max} = 1080 nm; see: Lawson, D. R.; Feldheim, D. L.; Foss, C. A.; Dorhout, P. K.; Elliot, M.; Martin, C. R.; Parkinson, B. *J. Electrochem. Soc.* **1992**, *139*, L68.

(25) Boulas, P. L.; Subramanian, R.; Jones, M. T.; Kadish, K. M. *Appl. Magn. Reson.* **1996**, *11*, 239.

(26) Kato, T.; Kodama, T.; Oyama, M.; Okazaki, S.; Shida, T.; Nakagawa, T.; Matsui, Y.; Suzuki, S.; Shiromaru, H.; Yamauchi, K.; Achiba, Y. *Chem. Phys. Lett.* **1991**, *186*, 35.

(27) Völkel, G.; Pöppl, A.; Simon, J.; Hoentsch, J.; Orlinskii, S.; Klos, H.; Gotschy, B. *Phys. Rev. B* **1995**, *52*, 10188.

(28) (a) Tsuda, M.; Ishida, T.; Nogami, T.; Kurono, S.; Ohashi, M. *J. Chem. Soc., Chem. Commun.* **1993**, 1296. (b) Schlueter, J. A.; Seaman, J. M.; Taha, S.; Cohen, H.; Lykke, K. R.; Wang H. H.; Williams, J. M. *J. Chem. Soc., Chem. Commun.* **1993**, 972. (c) Komatsu, K.; Murata, Y.; Sugita, N.; Takeuchi, K.; Wan, T. S. M. *Tetrahedron Lett.* **1993**, *34*, 8473. (d) Lamparth, I.; Maichle-Mössmer, C.; Hirsch, A. *Angew. Chem., Int. Ed. Engl.* **1995**, *34*, 1607.

(29) Mikami, K.; Matsumoto, S.; Tonoi, T.; Ohkubo, Y.; Suenobu, T.; Fukuzumi, S. *Tetrahedron Lett.* **1998**, *39*, 3733.

(30) de Coulon, V.; Martins, J. L.; Reuse, F. *Phys. Rev. B* **1992**, *45*, 13671.

(31) (a) Orbach, R. *Proc. Phys. Soc. London* **1961**, *77*, 821. (b) Abragam, A.; Bleaney, B. *Electron Paramagnetic Resonance of Transition Metal Ions*; Clarendon: Oxford; 1970.

(32) At low temperatures below 70 K, the ΔH_{msl} value becomes temperature independent because it is mainly determined by the inhomogeneous width of the powder spcetrum caused by the *g*-factor anisotropy.[27]

(33) (a) Eaton, S. S.; Kee, A.; Konda, R.; Eaton, G. R.; Trulove, P. C.; Carlin, R. T. *J. Phys. Chem.* **1996**, *100*, 6910. (b) Zhou, Y.; Bowler, B. E.; Eaton, G. R.; Eaton, S. S. *J. Magn. Reson.* **1999**, *139*, 165.

(34) Douthwaite, R. E.; Brough, A. R.; Green, M. L. H. *J. Chem. Soc., Chem. Commun.* **1994**, 267.

(35) Khaled, M. M.; Carlin, R. T.; Trulove, P. C.; Eaton, G. R.; Eaton, S. S. *J. Am. Chem. Soc.* **1994**, *116*, 3465.

(36) MO calculations of the radical anion of 1,4,10,24-$(C_6H_5CH_2)_4C_{60}$ with the unrestricted Hartree−Fock (UHF) formalism would have been preferred but unfortunately the SCF field could not be obtained in the calculation.